Stockholm University

Master Thesis

Degree Project in
Geology 60 hp

Differential preservation of high-P rocks coupled to impermeable layer and availability of fluids during metamorphism, in (CBU) Syros, Greece

Niklas Strandberg

Stockholm 2019

Department of Geological Sciences
Stockholm University
SE-106 91 Stockholm

Table of Contents

Abstract

A layered sequence of eclogite, blueschist and greenschist, belonging to the Cyclades Blueschist Unit (CBU), crops out in a meter-high vertical sea cliff on SE Syros. Here, I show that the sequence records local scale preservation of eclogite, which was formed at 2.0 GPa and 550 °C and was shielded from retrogression at blueschist facies conditions (1.6 Gpa and 510°C) by an impermeable layer of metasandstone. That this preservation was likely a result of limited fluid availability during retrogression is indicated by petrological observations of partial hydration of the eclogite at its boundary with the blueschist. The blueschist is further retrogressed at greenschist facies conditions, the extent of which correlates with distance from the metasandstone. I suggest that the preservation of the sequence reflects a lack of fluid during periods of metamorphism preventing alteration of the high-*P* rocks. The P-T estimations and relative timing of the alteration events are consistent with previous studies of the SE part of Syros.

Introduction

A consequence of plate tectonics is plate convergence, manifested as collision of continental plates or subduction of oceanic lithosphere and formation of volcanic arcs. During subduction, an oceanic plate bends and submerges into the asthenosphere. This is the recycling system of plate tectonics. The average rate of subduction is estimated to be 62 km per million years (Royden and Husson., 2006; Ring et al., 2010). The process creates unique metamorphism conditions, forming high-pressure and low-temperature rocks (HP-LT rocks). These conditions arise because wet oceanic slabs heat slowly but responds more rapidly to pressure changes. The subducted rock can be metamorphosed at blueschist and eclogite facies conditions; facies which are characterized by specific mineral assemblages (Poli and Schmidt., 2002). Metamorphism follows a so-called pressure temperature path (P-T path). This contains three stages: I) Prograde metamorphism, during which temperature increases, II) Peak metamorphism, at which the highest temperature is reached, III) Retrograde metamorphism, during which temperature decreases. P-T paths are deduced from rocks that make it back to the surface. However, most subducted rocks never do and are instead assimilated into the mantle (Ring et al., 1999). On rare occasions, HP-LT rocks are exhumed to the surface, although the majority of these rocks experience some retrogression. Thus few HP-LT rocks are preserved (Ernst, 1988). Exhumation itself describes the displacement of rocks relative to the surface (England and Molnar., 1990). Exhumation is comprised of three processes: normal faulting, ductile thinning and erosion (Ring et al., 1999), which tend to act in concert with one another (Platt, 1993).

Various mechanisms have been put forward to explain the preservation of HP-LT rocks. Of these mechanisms, fluid flow or the lack of fluid flow is often favoured (Matthews and Schliestedt, 1984; Proyer, 2003; Breeding et al., 2003; Beinlich et al., 2010; Kleine, et al., 2014; Schorn, 2018). Periods during which rocks are isolated from fluids can result in no metamorphism occurring even if the P-T conditions are appropriate for metamorphism to occur (Proyer, 2003; Schorn, 2018). For the same reason, fluid paths have been found to be an important factor controlling the preservation of HP-LT rocks. For example, channelizing features such as rock-contacts and shear zones localize fluid flow and can affect the distribution of HP-LT assemblages (e.g. Breeding et al., 2003). Also impermeable layers e.g. marbles, can locally shield HP-LT rocks from fluids allowing their preservation (Matthews and Schliestedt,

1984). Metasomatic changes of host rock chemistry caused by fluid-rock interaction can result in formation of HP-LT assemblages (Beinlich et al., 2010). Also, fluids can stabilize HP-LT assemblages during retrogression (Kleine, et al., 2014).

Protolith composition can also affect the distribution of HP-LT assemblages. For example, interlayered eclogite and blueschist facies rocks can form at the same P-T path conditions in rocks of different bulk compositions (Beinlich et al., 2010; Brovarone et al., 2011; Wei and Clarke., 2011; Skelton et al., 2019).

This project concerns the competing roles of P-T conditions, protolith composition as well as fluid flow and fluid composition in preserving HP-LT rocks. The locality chosen for this project; the Fabrika shore on Syros (Greece), provides a unique opportunity to study these processes. Here, previous work has shown preservation of blueschist in greenschist facies rocks caused by CO_2-bearing fluid (Kleine et al., 2014) and that eclogite and blueschist have formed at the same P-T conditions in rocks of different bulk compositions (Skelton et al., 2019). The focus of the project is a layered sequence comprising an impure metasandstone and metamorphosed mafic rocks. Here, eclogite, blueschist and greenschist occur in close proximity to one another. This site is located a few meters from the locality which was studied by Kleine et al. (2014). The study reported here is part of a bigger project which aims to elucidate the preservation of the HP-LT rocks along the Fabrika shore. In the study, petrographic and geochemical analyses as well as thermodynamic modelling will be used to find out how eclogite, blueschist and greenschist were preserved in close proximity to one another.

Regional geology

The Hellenides and Aegean Sea

The Hellenides system is located between Greece and Turkey (Figure 1a), and is shaped by the convergence of the Eurasian Plate and African Plate which has been ongoing since the late Mesozoic (Aubouin., 1957; Jacobshagen et al., 1986; van Hinsbergen et al., 2005). The convergence led to subduction of the Hellenic slab which consisted of a smaller continental block, ophiolites and oceanic units (Bonneau, 1984). During subduction, the upper parts of these blocks and units were successively detached. This led to the formation of a nappe stack of these units on top of the Eurasian plate (Ricou et al., 1998). The nappe stack has been analysed to reconstruct the tectonic evolution of the region (Ricou et al., 1998; van Hinsbergen et al., 2005). This has led to the following north to south subdivision of the Hellenides along the Aegean transect: 1) the Srednogorie Block and Rhodope-Sakarya Block, 2) the Vardar-Izmir Oceanic Unit, 3) the Peagonian-Lycian Block, 4) the Pindos Oceanic Unit (including the Cycladic Blueschist Unit), 5) the Tripolitza Block, 6) the Ionian Block, and 7) the East Mediterranean Ocean (Ring et al., 2010). This study focuses on the part of the Pindos Oceanic Unit which crops out on Syros. This unit formed between ~55 and 30 Ma in an accretionary setting (Ring et al., 2010). It stretches from northwestern to southeastern Greece (Pindos nappe) and includes the Cycladic Blueschist Unit. The unit is below the Pelagonian block and above the Tripolitza Block (Bonneau, 1984; Jolivet et al., 2013). The Pindos Oceanic Unit is the remains of the subducted Pindos Sea (Bonneau, 1984).

The process of slab retreat started during Eocene subduction of the Pindos Unit (Faccenna et al., 2003; Thomson et al., 1998), and was initiated by subduction of small continental lithosphere blocks (Brun and Faccenna, 2008). Slab retreat describes the motion of the subduction zone in the opposite direction of the slab moment, hence the subduction front moving backwards (Ring et al., 2010). The Hellenic slab subduction zone is retreating towards the African Plate. Slab retreat led to arc magmatism (Fytikas et al., 1984; Pe-Piper et al., 2002) and subduction metamorphism moving southward (Ring et al., 2010; Jolivet et al., 2013).

Syros

The rocks on Syros belong to the Cyclades Blueschist Unit (CBU), located in the back arc of the Hellenic subduction zone. The majority of rocks on Syros have or had a HP-LT mineral assemblage. The CBU on Syros can be divided into two lithological sequences: 1) a lower sequence consisting of volcano-sedimentary rocks, metabasalts, marble and metavolcanics, and 2) an upper sequence that consists of metabasalt and ohpiolitic mélange (Keiter et al., 2011).

The ages of metamorphism differ between the lower and upper sequence. The HP-LT event in the upper sequence is dated to ~52 Ma (Tomaschek et al., 2003) or 53 to 46 Ma (Cliff et al., 2017), and to 42 Ma to ~30 Ma (Cliff et al., 2017) or 43 to 38 Ma (Skelton et al., 2019) in the lower sequence. Peak metamorphism of the CBU is estimated to have occurred at ~500 °C and 1.5-1.6 GPa (Schumacher et al., 2008). In a recent study, Skelton et al. (2019) estimated peak metamorphic conditions of 1.5 - 2.1 GPa and 520-580 °C for HP-LT rocks from the Fabrika shore on SE Syros. These authors also suggested that the CBU could be a stacked nappe explaining different ages.

The HP-LT rocks on Syros are partly overprinted at greenschist facies conditions. The timing of this retrogression is poorly constrained, with an $^{40}Ar/^{39}Ar$ age of ~30 Ma (Maluski et al., 1987) and a Rb –Sr age of ~35- 20 Ma (Bröcker et al., 2013). Skelton et al. (2019) found greenschist retrograde metamorphism to have ended ~27 Ma. They estimated a pressure of 0.34 ± 0.21 GPa and a temperature of 450 ± 68 °C for this event.

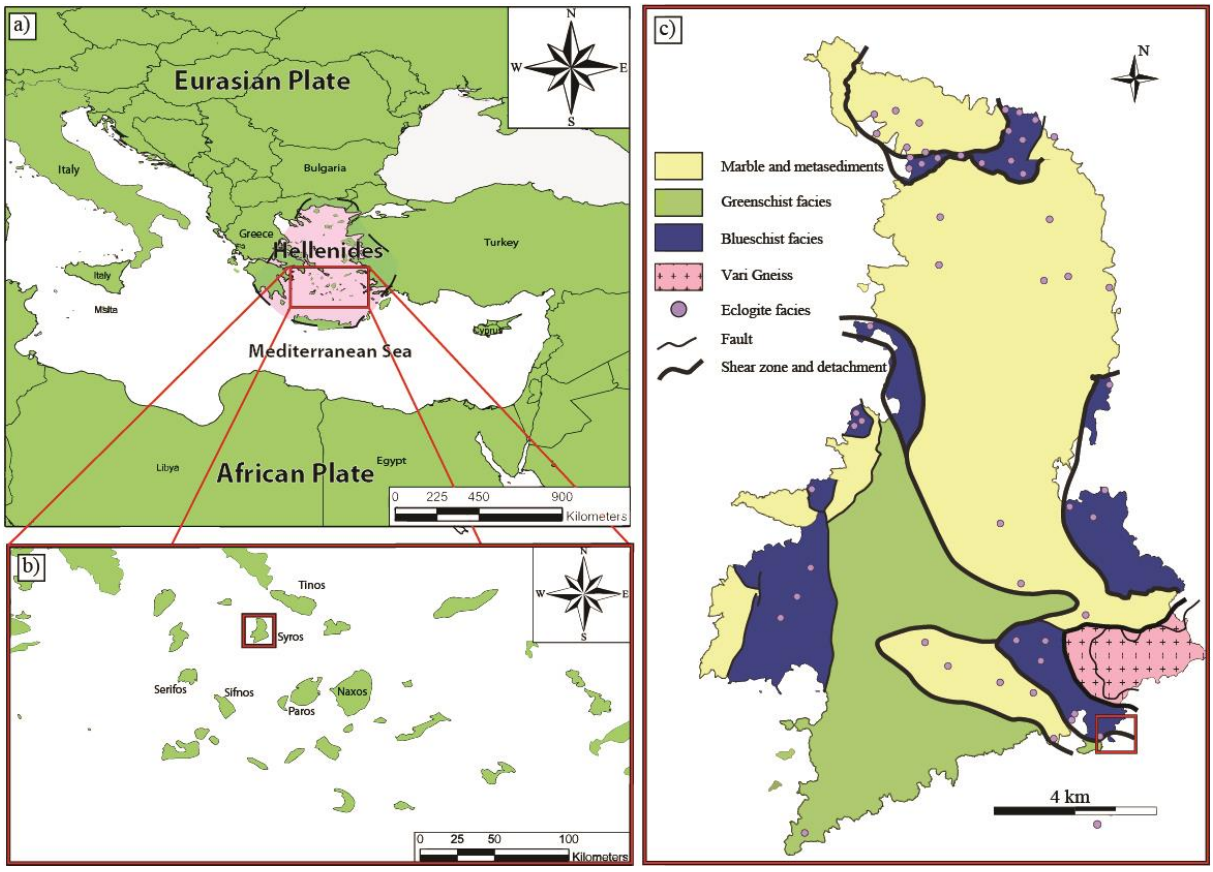

Figure 1. a) Regional map of Eastern Mediterranean displaying the Hellenides system extent, made in Arcgis, country borders data from https://www.naturalearthdata.com/. b) displays Cyclades archipelago, red box displays Syros location. (c) Geological map of apparent metamorphic grade Syros edited from Skeleton et al. (2019).

Fabrika

The study was undertaken at a locality on the Fabrika shore. This shore is located along the southeastern coast of Syros (Figure 1c). Here, an exceptional amount of pristine HP-LT rocks crop out along the shore. The rocks at Fabrika, classified according to their appearance in the field are eclogite, blueschist, greenschist and impure metasandstone.

The rocks form a layered sequence, with layer thicknesses ranging from tens of meters to decimetres (Figure 2). Some parts of the sequence are homogenous in terms of apparent metamorphic facies whereas other parts comprise interlayered greenschist and/or blueschists and/or eclogite layers (Figure 3a). Skelton et al. (2019) showed that the blueschist and eclogite experienced the same P-T conditions, with the mineral assemblage being controlled by bulk chemistry. Kleine et al. (2014) showed that preservation of blueschist in greenschist was controlled by fluid chemistry. The mixture of greenschist, blueschist and eclogite layers shows that preservation and alteration were heterogeneous in area. Along the shoreline is a poorly exposed section along which ultramafic knockers are found (Skelton et al., 2019). These authors infer that this section could be a mélange which channelized fluids that may have contributed to large variation of preservation of HP-LT rock along Fabrika shore.

There is a mixture of brittle faults and ductile shear zones along the Fabrika shore with the type of deformation appearing to be dependent on the rock type. The eclogite behaved in a stiff manner during deformation, exhibiting brittle faulting whereas the blueschist behaved in a more ductile manner, exhibiting shearing (Figure 3b). Most faults and shear zones dip north (Figure 2). Some of them are in between the different rock-types suggesting that juxtaposition of the layers could have occurred. There are clear indications of a late stage carbonation event inferred from carbonate rich veins, especially in the northern part of the shore. The veins intrude eclogite and blueschist unit and have a rusty appearance and are therefore likely to contain siderite or dolomite.

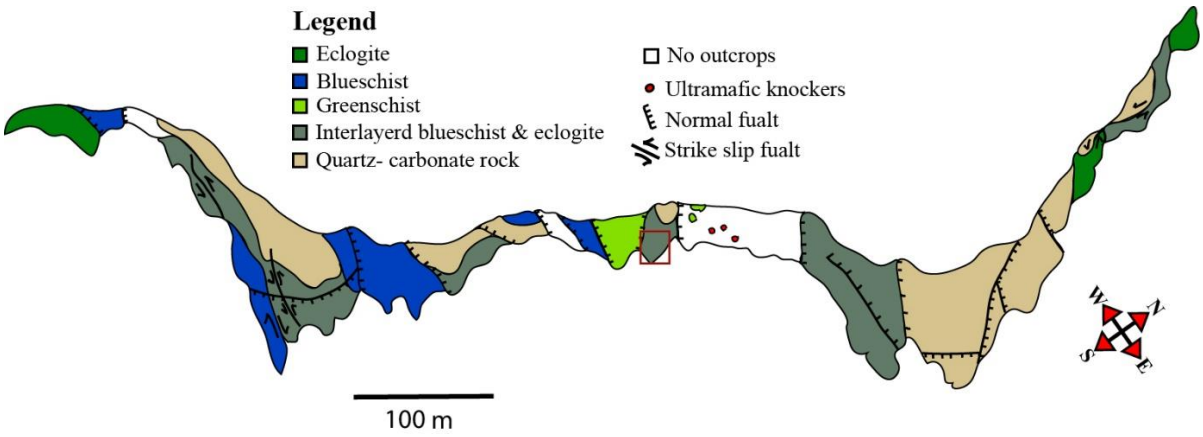

Figure 2. Geological map of Fabrika shore focused on metamorphic facies. Interlayered eclogite and blueschist are grouped into one unit, to difference the pure blueschist, eclogite from interlayered mixtures. Red square shows the location of the outcrop which this report focuses on (Figure 4). The area was mapped during the course Geodynamics, during a period from 21-27 October 2018.

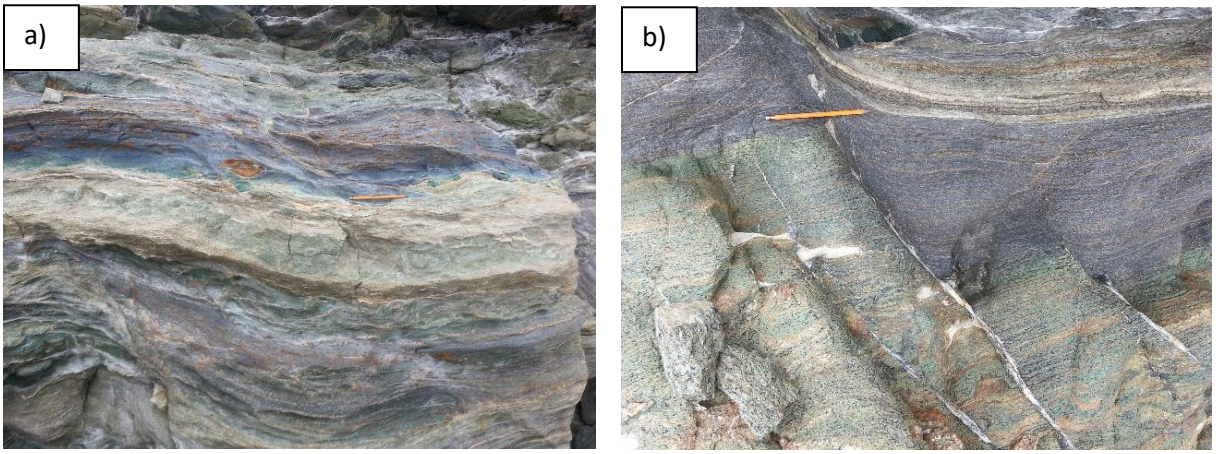

Figure 3. a) An example of interlayered blueschist and eclogite found at Fabrika. b) Eclogite and blueschist layer cut by multiple faults. With the eclogite being brittle and blueschist ductile, were blueschist shows internal deformation bending upwards near the fault.

Method

A total of five samples were collected from an outcrop at Fabrika shore at N 37°23,332, E 24°57,197 (Syros, Greece). These samples were chosen in order to capture the various rock types and transitions between them. Therefore, a sample of each of the following rock types was collected; metasandstone, eclogite, eclogite-blueschist transition, blueschist-greenschist transition and greenschist. The samples vertical positions refer to the contact between eclogite and metasandstone (Figure 4). The samples are named as follows:

18/SY/01/NS Greenschist, located 32 cm bellow contact.
18/SY/02/NS Blueschist greenschist transition, located 23 cm bellow the contact.
18/SY/03/NS Blueschist, located 18 cm bellow contact.
18/SY/04/NS Eclogite blueschist transition, located 6 cm bellow contact.
18/SY/05/NS Impure metasandstone located 2 cm above contact.

The five rocks collected were prepared for the making of thin sections by cutting to 4 x 2 x 1 cm blocks, at Stockholm University. The samples were sent to Canada for production of thin sections. Two thin sections were made from each of rocks 18/SY/03/NS and 18/SY/04/NS, increasing the number of samples to seven. The thin sections are referred to as SYNS 01 – 05 and are correlated to the rocks in the following way;

18/SY/01/NS -> SYNS 01
18/SY/02/NS -> SYNS 02
18/SY/03/NS -> SYNS 03a + SYNS 03b
18/SY/04/NS -> SYNS 04a + SYNS 04b
18/SY/05/NS -> SYNS 05

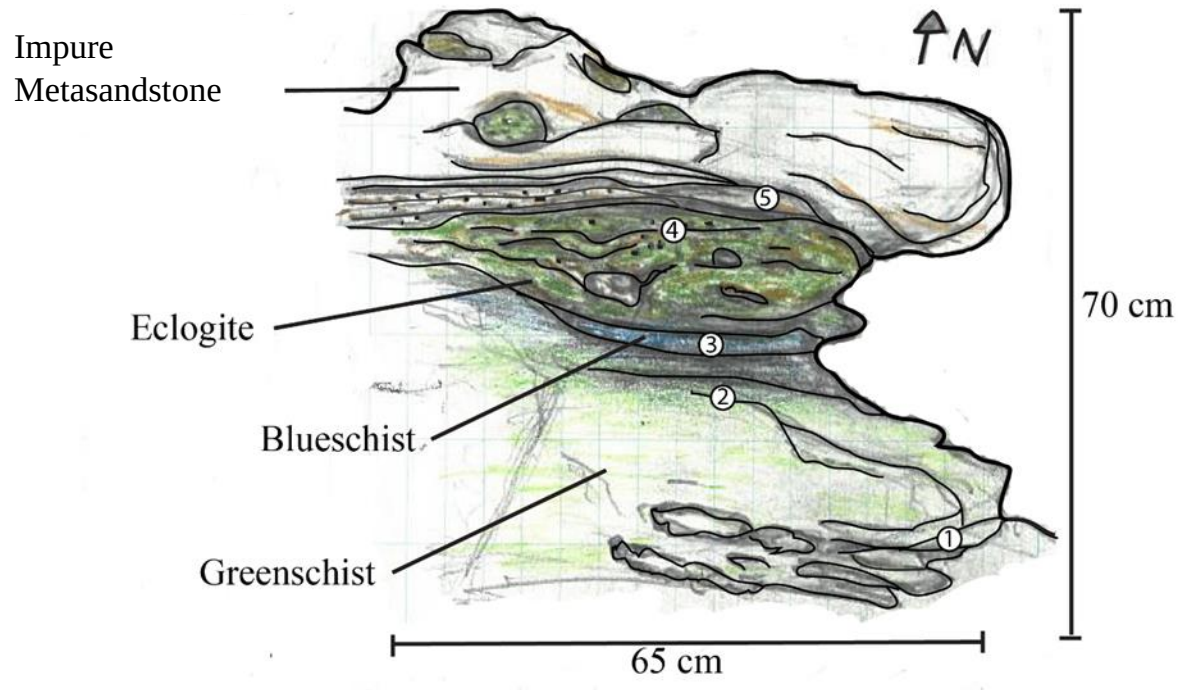

Figure 4. Digitalized sketch of sampled outcrop at Fabrika, labelling the five sample locations. Illustrated from a perpendicular viewpoint were the impure metasandstone is highest above sea level. The labelled numbers are corresponding for the samples 18/SY/01/NS to 18/SY/05/NS with the same number as in illustration, for example point (1) on illustration are sample location for 18/SY/01/NS.

XRF

The eclogite, blueschist, greenschist and impure metasandstone were prepared for XRF analysis at Stockholm University, using a rock crusher then a mill to turns the rock into a fine powder. The samples were shipped to Activation Laboratories (Actlabs) in Canada. The samples were analysed for major (oxides) and trace elements separately. Prior to fusion, the samples were cooked at 1000 °C for two hours. Loss of ignition (LOI) was given by the resultant weight loss for each of these samples. The major elements were analysed using the heavy absorber fusion technique of Norrish and Hutton, (1969). The roasted samples (0.75g) were mixed with releasing agents (9.75 g): lithium metaborate, lithium tetraborate and lithium bromide. The samples were analysed with a Panalytical Axios Adveanced wavelength dispersive XRF, using the standard G-16 for calculations. The detection limit is about 0.01% for most elements. The trace element analysis was done on compressed pellets which contained 6 g of each sample. The mass absorption were determined by measuring the Compton scatter of the Rh-tube (e.g., Nisbet et al., 1979). The background and mass absorption corrected intensities were calculated relative to a calibration constructed from 24 geological reference materials. The samples were analysed on a Panalytical Axios Advanced using the Protract program and the detection limit for the elements was generally between 1 and 5 ppm.

Point counting

Point counting was used to quantify the mineral assemblages of the samples. In this method, mineral identifications at evenly spaced points throughout the thin section are used to estimate mineral percentages (modes) for the sample. Five hundred points were counted in order get statistically useful values. In thin sections SYNS03a and SYNS03b, which contain both eclogite and blueschist, 500 points were counted for each part of the section. The software PelaconPointCounter9 was used for point counting. The software moves the thin section stage horizontally by a predetermined distance, here 0.5 mm. The vertical position is maneuvered manually. At each point, a mineral identification was made using a Leica microscope. The results were compiled and normalized to 100 %. The modal data standard error was calculated with formula developed by Van der Plas and Tobi, (1965).

$$\boldsymbol{\sigma = \sqrt{\frac{p(100-p)}{n}}}$$

p = the mineral mode.
n = the total numbers of point counted.

Electron Micro Probe Analysis (EMPA)

The samples SYNS01 (Greenschist), SYNS03a (blueschist-eclogite) and SYNS04a were analysed with an electron micro probe analyser (EMPA) at Oslo University. Electron microscopy is a none destructive method used to determine chemical composition of minerals on a micro scale. It works by shooting a focused electron beam on samples, resulting in emission of X-ray spectra that are characteristic for the chemical composition. The samples were carbon coated and analysed with a Cameca Sx 100 EMPA. The settings used for the analysis were an accelerating voltage of 15 kilovolt (kV), a beam current of 15 nA and counting peak time of 10 seconds. The standards used for calibration are listed in table 1.

Table 1. Standards used for calibration

Wollastonite	Ca, Si
Albite	Na
Orthoclase	K
Pryofanit	Ti, Mn
Pure iron	Fe
Chromium (III) oxide	Cr
Aluminum oxide	Al
Magnesium oxide	Mg

Average pressure and temperature

Mineral compositions determined by EMPA were used for calculating activities of the mineral end members. The calculations were done in the program AX62 which uses the database of Holland and Powell (2011). The activity for the minerals were entered in THERMOCALC 3.33 to estimate average pressure and temperature conditions using the built in average PT method (Powell and Holland, 1994). The method returns an estimate of the average pressure and temperature of peak metamorphism as well as a diagnostic parameter for uncertainty: σ_{fit}. The value of σ_{fit} is a measurement of the consistency between the P-T estimation and the input data. Other diagnostic parameters (e* and hat) are used to identify mineral end members which are poorly constrained. By systematically removing these mineral end members as satisfactory value of σ_{fit} is obtained for which confidence of the average P-T estimation is better than 95%. The system was simplified by assuming that the only fluid present was H_2O, by setting X_{H2O} = 1 in the model.

Results

Mineral Abbreviations

The following mineral abbreviations are used: **carb**: carbonate (dolomite and calcite (cc)), **ep**: epidote, **gl**: glaucophane, **phg**: phengite, **chl**: chlorite, **alb**: albite, **grt**: garnet, **omp**: omphacite, **qtz**: quartz, **ti**: titanite, **rt**: rutile.

The studied profile is ca. 0.7 m long and the rock types identified along this profile, based on appearance in the field are classified as eclogite, blueschist, greenschist and impure metasandstone (Figure 1).

SYNS 01 – Greenschist

The greenschist has a dull green colour with albite occurring as grey spots. The rock contains chlorite, white mica, partly altered 1-3 mm garnets which are red in colour, and 0.5- 1 cm long prismatic crystals of epidote.

The mineral assemblage seen in SYNS 01 thin section is: garnet (0.4 ± 0.6 %) + glaucophane (0.4 ± 0.6 %) + white mica (2.8 ± 1.5 %) + chlorite (25.4 ± 3.9 %) + epidote (11.8 ± 2.9%) + albite (41.2 ± 3.9%) + carbonate (13.8 ± 3.1 %) + rutile (>1%), (appendix 1). SYNS 01 was classified by field appearance as a greenschist, which is reasonable with the high quantities of chlorite. The sample could also be identified as a retrogressed HP-LT rock, based on the occurrence of the HP-LT minerals: glaucophane, phengite and garnet. That these minerals are unstable is inferred because glaucophane is partly replaced by chlorite (Figure 5a), and garnet

is replaced by albite and chlorite. It is thus concluded that the greenschist was previously a HP-LT rock and that it underwent retrogression at greenschist facies conditions.

The white mica in the sample is a mixture of phengite and muscovite, where HP phengite are partly replaced by muscovite (Figure 5d). The sample contains two generations of epidote. The first generation are large with anomalous interference colours, with bladed crystals aligned to foliation. The second generation of epidotes are small crystals with tabular shapes. The pristine nature of some epidotes indicate their stability (Figure 5b). However other epidotes crystals are fractured with pull apart textures (Figure 5c). The gaps created in between are filled by calcite, indicating a late stage carbonation of the rock. The extent of carbonation was extensive with 13.8 % of the sample being calcite.

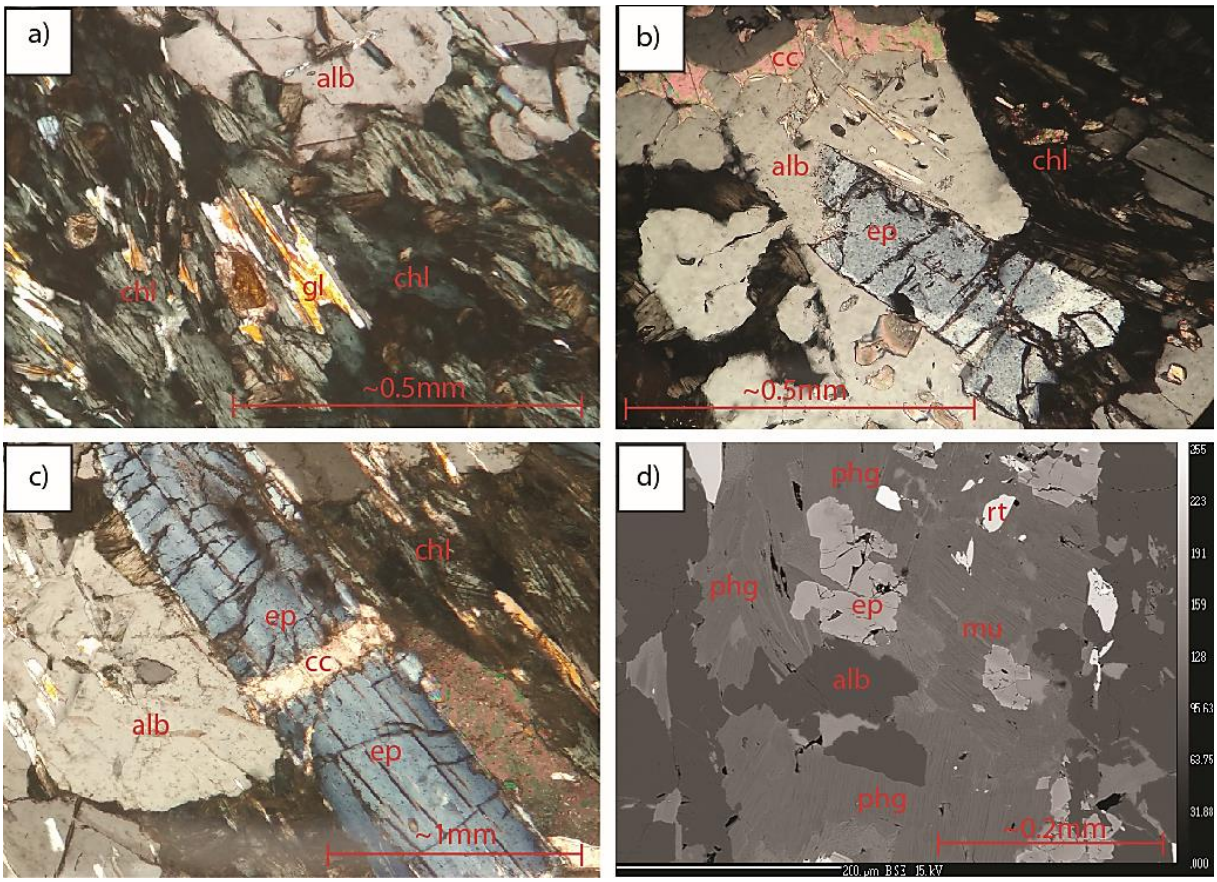

Figure 5. Pictures of minerals in SYNS01: a) Glaucophane (gl) being replaced by chlorite (chl), with the glaucophane displaying shallows tail texture. b) Epidote (ep) partly replaced by albite (alb) along the mineral c axis, while remaining axis appear stable seen as the albite has grown around it without any additional reaction. c) A fractured epidote has been pulled apart, seen as simulations extinction of the epidote, the gap has later been filled by calcite. d) The white mica in SYNS01 are a mixture of phengite (phg) and muscovite (mu), with phengite partly replaced by muscovite. SEM photo of white micas.

SYNS 02 – Greenschist-Blueschist transition

The transition between blueschist and greenschist is gradual and occurs over a distance of ~5-10 cm. The sample (SYNS 02) taken from this transition contains: garnet (> 0.1%) + glaucophane (14.8 ± 3.2 %) + phengite (14.8 ± 3.2%) + chlorite (7.0 ± 2.3 %) + epidote (23.2 ± 3.8%) + albite (18.0 ± 3.4 %) + actinolite (16.4 ± 3.3 %) + carbonate (1.8 ± 1.2 %) + rutile (<1 %) (appendix 1). Sample SYNS02 has the same mineral assemblage as sample SYNS 01, although significant differences in some modes, especially of phengite, glaucophane, chlorite, epidote and calcite. It is inferred that SYNS 02 experienced less retrogression than SYNS 01

based on lower amounts of chlorite and albite. Glaucophane crystals have weak blue to purple pleochroism. They are partly replaced by albite (Figure 6a). The epidote characteristics are similar to those of epidote in sample SYNS 01, with anomalous interference colours, brittle fractures and pull apart structure. Epidote is partly replaced by chlorite (Figure 6b). The sample lacks foliation.

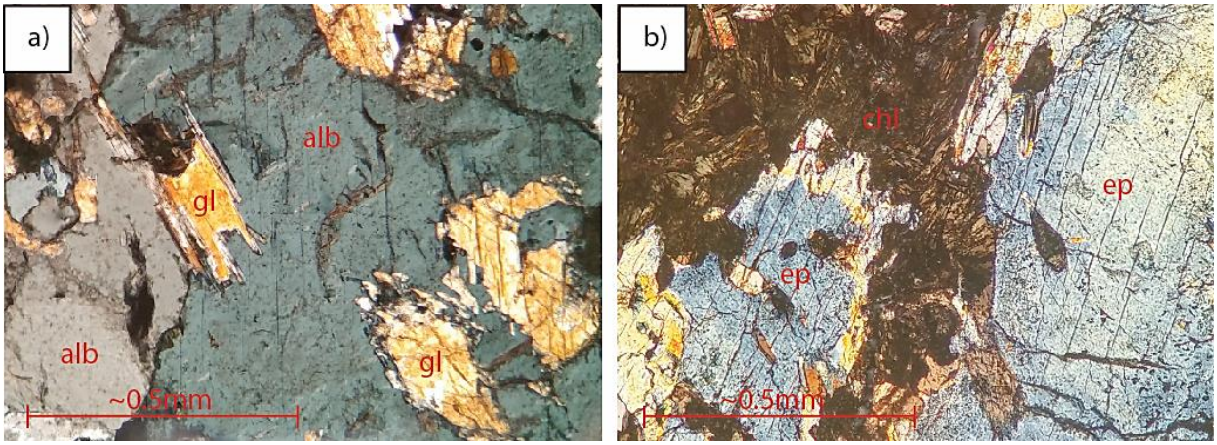

Figure 6. a) Glaucophane (gl) being partly replaced by albite, glaucophane displays shallow trail texture (left mineral) and fractured replacement (right mineral). b) Epidote (ep) being partly replaced by chlorite (chl).

SYNS 03a and 03b- Blueschist-Eclogite transition

The transition from eclogite to blueschist is sharp and seen as a strong colour change from green to blue in hand specimen. The blueschist has a fine-grained matrix of pristine glaucophane, which gives the rock a deep blue colour.

The thin sections SYNS 03a and SYNS 03b (from same rock) capture the sharp transition from blueschist to eclogite. Mineral modes were calculated separately from blueschist and eclogite parts of the samples. The blueschist parts of thin sections SYNS 03a and SYNS 03b are combined to one mode and the eclogite parts of these sections are also combined to one mode. The blueschist is further subdivided into mixed assemblage and glaucophane rich zones (Figure 7). The eclogite part is subdivided into phengite rich and omphacite rich zones.

SYNS 03a & 03b - Blueschist

The blueschist parts of samples SYNS 03a and b contain: garnet (1.0 ± 0.6 %) + glaucophane (31.5 ± 2.9 %) + phengite (32.7 ± 3.0 %) + chlorite (1.0 ± 0.6) + epidote (20.1 ± 2.5 %) + albite (8.6 ± 1.8 %) + carbonate (< 1 %) + rutile (< 1 %) + titanite (< 1 %) + omphacite (2.0 ± 0.9 %) + lawsonite pseudomorph (< 1 %) (appendix 1). Phengite and glaucophane are partly replaced by chlorite (Figure 8a).

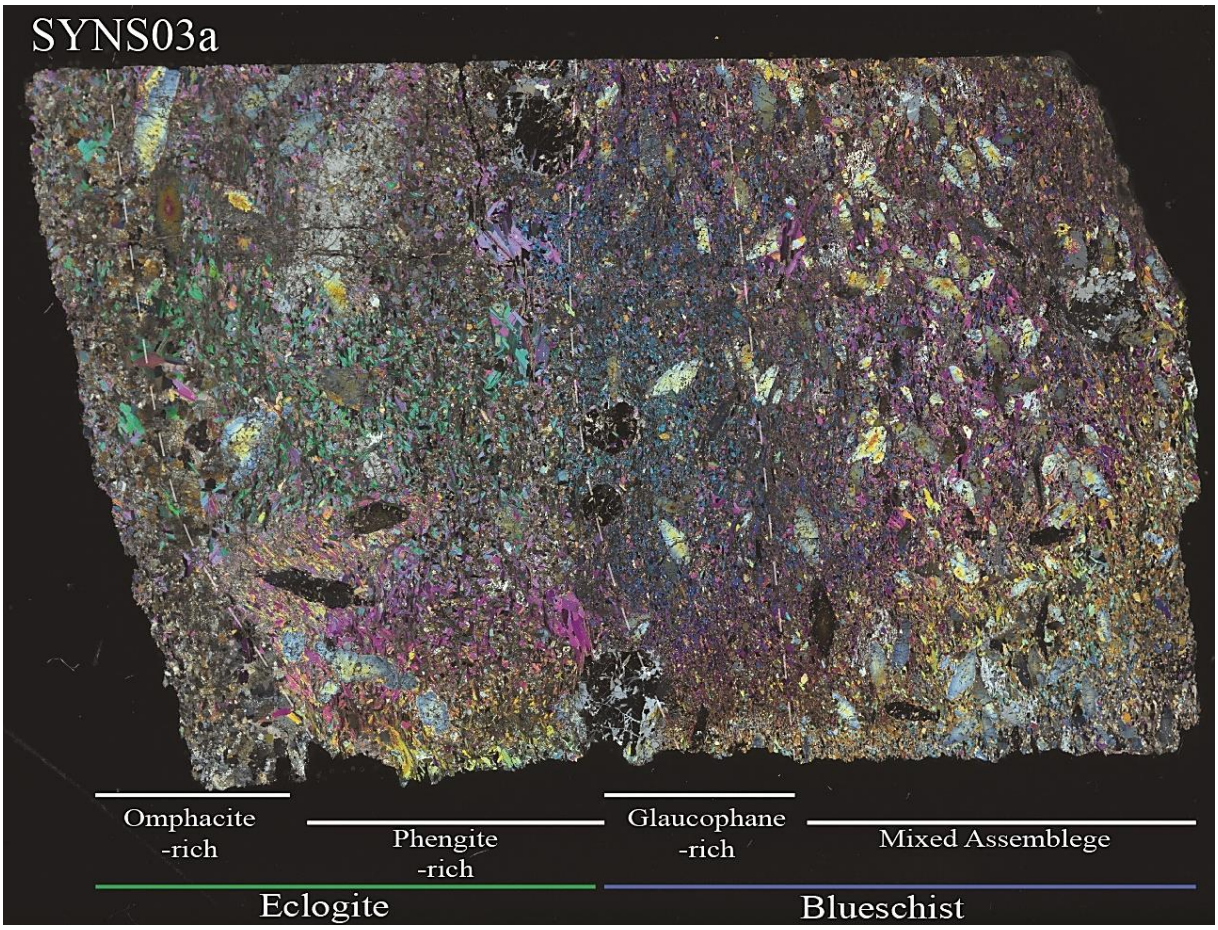

Figure 7. Sample SYNS03a thin section scan in XPL displaying the eclogite-blueschist transition. The eclogite is further divided into omphacite and phengite rich zones. The blueschist is further divided into glaucophane rich and mixed assemblage zones. The whole sequence is 2.6 cm long.

SYNS 03a & 03b – Eclogite

The eclogite parts of samples SYNS 03a and b contain: garnet (0.8 ± 0.6 %) + glaucophane (0.9 ± 0.6 %) + phengite (50.1 ± 3.2 %) + chlorite (0.4 ± 0.4 %) + epidote (18.8 ± 2.5 %) + albite (4.3 ± 1.3%) + clinozoisite (5.8 ± 1.5 %) + calcite (1.4 ± 0.7 %) + rutile (< 1 %) + titanite (< 1 %) + omphacite (16.2 ± 2.3 %) + lawsonite pseudomorph (< 1 %) (appendix 1). The following reactions were found: garnet partly replaced by chlorite; glaucophane replacing omphacite (Figure 8b); phengite replaced by albite (Figure 8c) and replacement of one generation of epidote (ep1) by a later generation (ep2) (Figure 8d). There are large Clinozoisite crystals (2 mm wide) present in the eclogite section of the samples, not found in the blueschist section. Foliation is seen by alignment of phengite, glaucophane and epidotes. The fractures are filled with carbonates (calcite or dolomite).

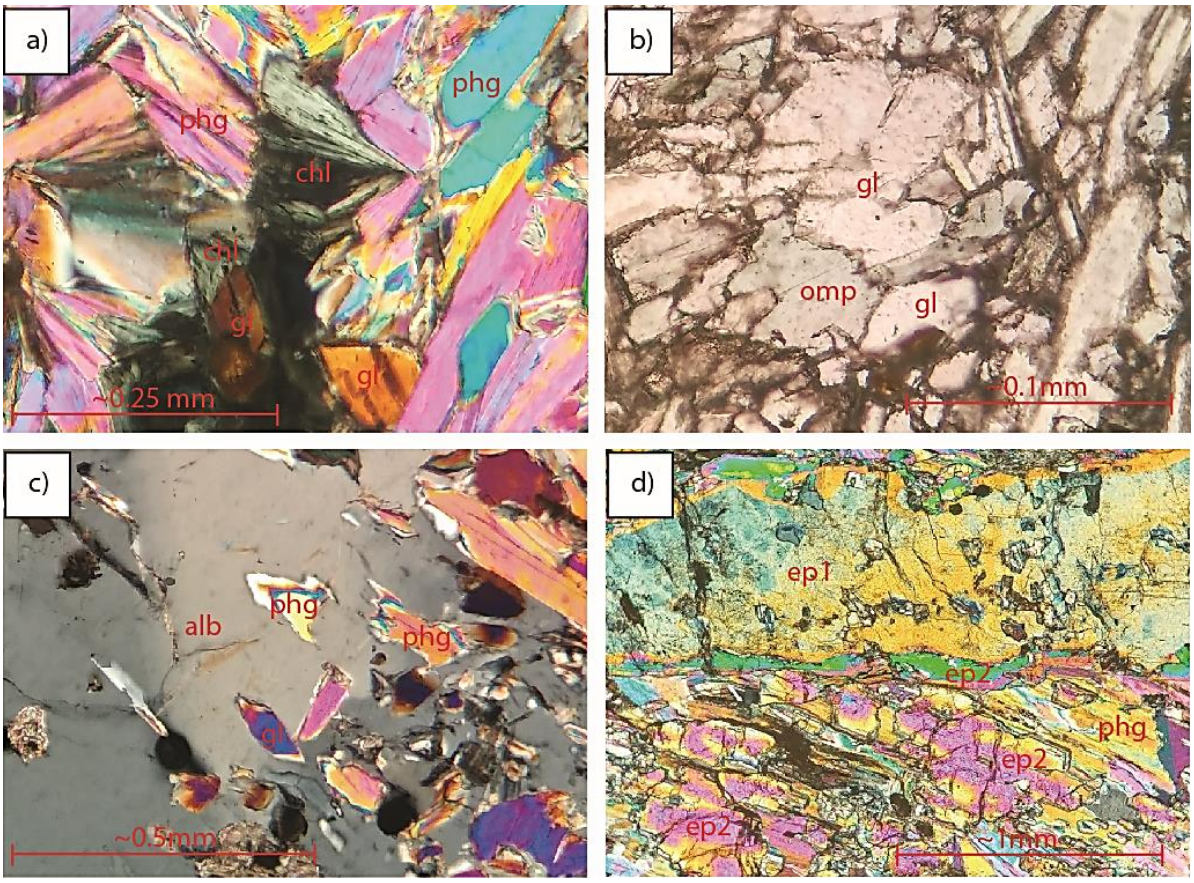

Figure 8. a) Phengite (phg) and glaucophane (gl) replaced by chlorite (chl), sample SYNS 03b blueschist part. b) Omphacite (omp) partly replaced by Glaucophane (gl), in sample SYNS 03b eclogite part. c) Enclosed phengite (phg) were partly replaced by albite (alb), glaucophane (gl) partly replaced by phengite (phg), SYNS 03a blueschist part. d) Large epidote (ep1) crystal with anomalus interference colours are zoned by epidote (ep2) with 3 order interference colour, sample SYNS 03a blueschist part.

SYNS 04a & 04b – Eclogite

The eclogite rock occurs in a pod shape that is about 15 cm in diameter and located immediately below the quartzite, from which it is separated by a few centimetres thick layer of dark garnet rich rock. The eclogite is fine-grained with a dark-green colour likely caused by omphacite. The rock contains 3 mm wide garnets and a 2-3 cm clast containing quartz and mica. Multiple beige veins that are likely dolomite or calcite crosscut the eclogite.

The thin sections SYNS 04a & 04b contain: garnet (8.3 ± 1.7 %) + glaucophane (3.0 ± 1.1 %) + phengite (27.8 ± 2.8 %) + chlorite (< 1%) + epidote (15.6 ± 2.3 %) + albite (10.7 ± 2.0 %) + calcite (0.8 ± 0.6 %) + rutile (<1 %) + omphacite (30.1 ± 2.9%) + lawsonite pseudomorph (< 1 %) (appendix 1). The rock is foliated. The field classification of the rock as an eclogite is validated by the abundance of pristine omphacite and garnet.

The thin sections contain evidence of the following reactions: lawsonite pseudomorph preserved in garnet (Figure 9a); garnet replaced by chlorite and albite; omphacite partly replaced by phengite (Figure 9b), and glaucophane (Figure 9c) phengite replaced by albite (Figure 9d); and one generation of epidote (ep1) replaced by another generation (ep2).

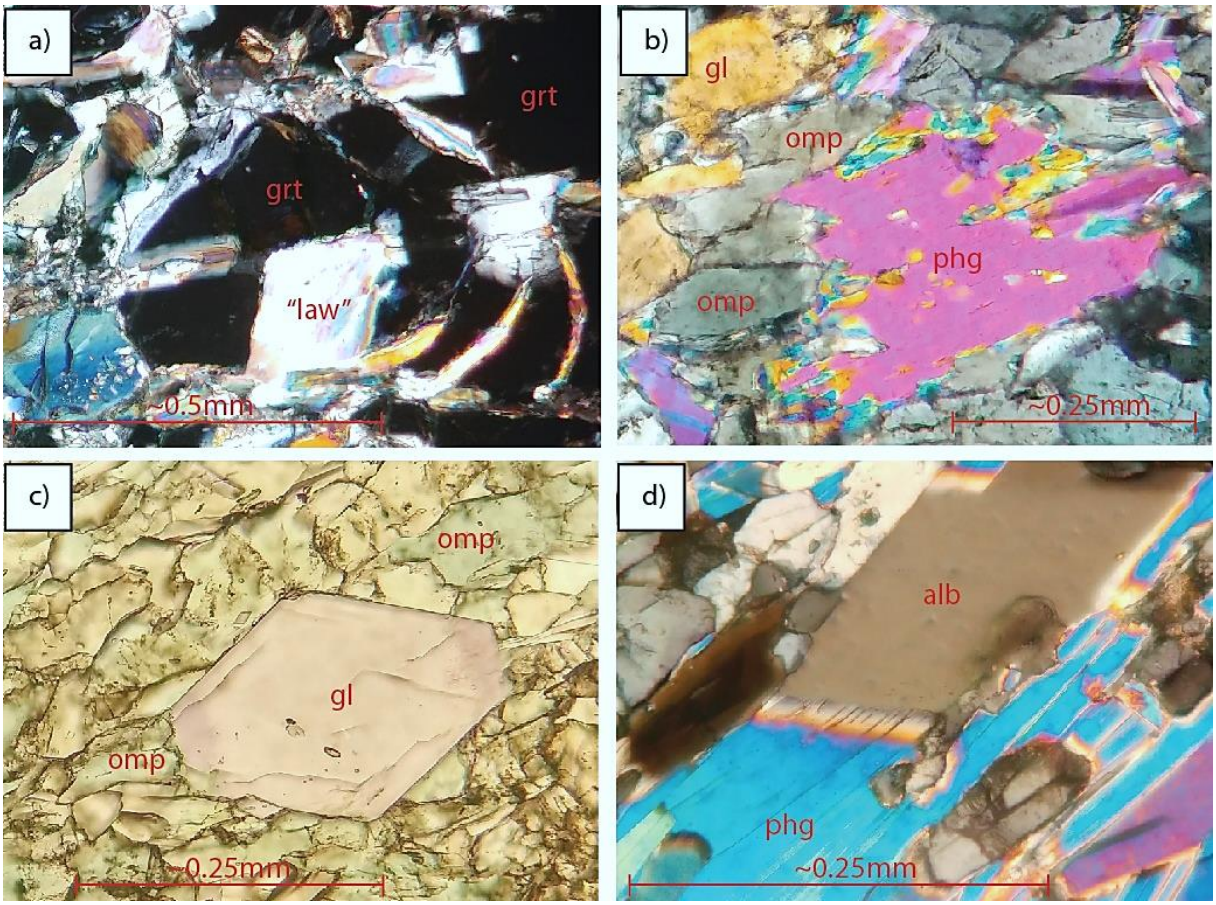

Figure 9. a) Lawsonite (law) pseudomorph in garnet (grt) still displaying the rhombical shape characteristic for lawsonite, in SYNS 04a. b) Omphacite (omp) crystals partly replaced by phengite (phg, in SYNS 04a. c) Omphacite (omp) crystals partly replaced by phengite (phg), in SYNS 04a. d) Phengite (phg) partly replaced by albite (alb), in SYNS 04b.

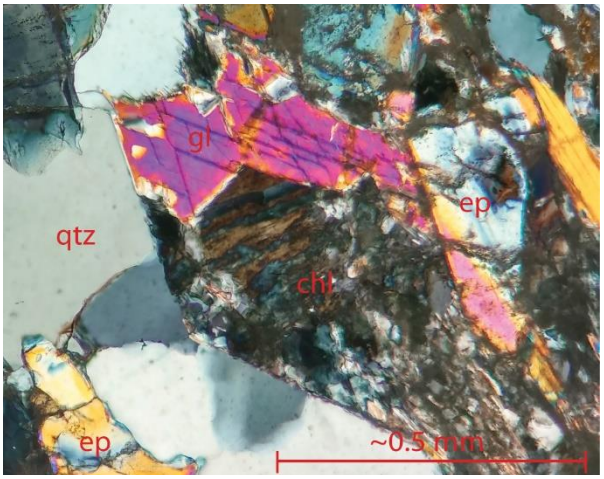

Figure 10. Glaucophane (gl) was partly replaced by chlorite (chl) retaining the c axis amphibole shape.

SYNS 07 – Impure Metasandstone

The rock has a white colour with a tint of brown. It contains fine-grained crystals of mica and quartz. It also contains a few pristine eclogite pods (Figure 4) that are garnet rich. The layer is about 35 cm thick and appears to pinch out towards the Northwest side of the outcrop.

The thin section contains: quartz (64.2 ± 4.3 %) + garnet (0.6 ± 0.7 %) + glaucophane (0.8 ± 0.8%) + phengite (20.8 ± 3.6 %) + chlorite (<1 %) + epidote (6.8 ± 2.3 %) + albite (3.6 ± 1.7 %) + carbonate (1.0 ± 0.9%) + rutile (<1 %) (appendix 1). The rock is foliated and some brittle fractures occur. Glaucophane are heavily retrogressed to chlorite (Figure 10) and phengite. Garnets are partly replaced by chlorite and albite, and one generation of epidote (ep1) is replaced by another generation (ep2).

Bulk chemistry

The bulk chemistry of the greenschist (SYNS 01 and 02) and the blueschist (SYNS 03) and eclogite (SYNS04) are rather similar, with greatest variation in LOI (Table 2).

	Greenschist SYNS 01	Greenschist SYNS 02	Blueschist SYNS 03a + b	Eclogite SYNS 04a + b	Impure Metasandstone SYNS 05
SiO2	44.56	48.69	49.86	51.96	76.8
Al2O3	17.82	16.69	17.52	14.64	10.00
Fe2O3(T)	7.49	8.04	8.20	6.91	4.20
MnO	0.18	0.12	0.11	0.13	0.08
MgO	6.47	6.68	6.21	5.35	1.38
CaO	9.76	7.85	7.69	10.64	3.02
Na2O	4.91	4.18	3.17	4.78	1.05
K2O	0.32	0.84	2.45	2.37	1.69
TiO2	1.49	1.58	1.73	1.38	0.23
P2O5	0.26	0.25	0.30	0.10	0.04
LOI	7.16	5.57	2.91	1.99	1.46
Total	100.4	100.5	100.1	100.3	99.95

Table 2. Major elements from XRF, given in weight percentage.

Microprobe data

The greenschist SYNS01, blueschist part of SYNS03a and eclogite SYNS04a were analysed, with the intent of using the data for average PT calculations. A minimum of three analyses of each mineral in the matrix was made, excluding quartz, rutile. The plagioclase was analysed in determining pure albite X_{ab} = 99.07 population. Cores and rims of zoned minerals (epidotes and garnets) were analysed.

White Mica

The white mica analyses in the blueschist (SYNS03a) and eclogite (SYNS04a) had Si and Mg + Fe contents corresponding to phengite (Figure 11a). The white mica in the greenschist (SYNS01) was a mixture of muscovite and phengite. It is thus inferred that HP-LT phengite was replaced by muscovite at greenschist facies conditions (Figure 5d).

	SYNS03a (blueshist)	Matrix phases				SYNS04a (eclogite)	Matrix phases			
	g (outer rim)	amp (gl)	cpx (om)	wm (phg)	ep	g (outer rim)	amp (gl)	cpx (om)	wm (phg)	ep
SiO_2	37.91	58.71	55.94	50.72	37.84	38.16	58.32	55.73	51.46	37.81
TiO_2	0.10	0.01	0.02	0.30	0.01	0.04	0.00	0.02	0.29	0.03
Al_2O_3	21.10	12.00	7.95	28.88	26.00	21.62	11.62	9.02	27.08	24.09
Cr_2O_3	0.02	-0.02	0.06	0.06	0.01	0.02	0.00	-0.02	0.03	0.03
Fe_2O_3	0.00	0.00	0.00	0.00	0.00	0.00	0.00	0.00	0.00	0.00
FeO	29.28	7.20	7.37	1.76	8.96	25.80	9.47	8.23	1.95	11.05
MnO	1.08	-0.04	0.25	-0.03	0.27	1.33	0.08	0.14	0.04	0.27
MgO	2.54	11.94	8.37	3.78	0.01	3.39	10.41	7.18	4.26	-0.02
CaO	8.24	1.11	14.01	-0.03	23.28	10.37	0.53	12.76	-0.04	23.51
Na_2O	0.05	7.01	6.43	0.67	0.02	0.04	7.25	7.48	0.38	0.01
K2O	0.00	0.02	0.02	10.64	0.00	0.00	0.07	0.02	10.67	0.01
Total	100.32	97.94	100.42	96.75	96.38	100.76	97.74	100.54	96.12	96.79
Oxygen	12	23	6	11	13	12	23	6	11	13
Si	3.00	7.91	2.00	3.33	2.99	2.97	7.95	1.99	3.40	3.00
Ti	0.01	0.00	0.00	0.02	0.00	0.00	0.00	0.00	0.01	0.00
Al	1.97	1.91	0.34	2.24	2.43	1.99	1.87	0.38	2.11	2.25
Cr	0.00	0.00	0.00	0.00	0.00	0.00	0.00	0.00	0.00	0.00
Fe3	0.02	0.06	0.10	0.00	0.57	0.07	0.09	0.17	0.02	0.73
Fe2	1.92	0.75	0.12	0.10	0.02	1.62	0.99	0.08	0.09	0.01
Mn	0.07	0.00	0.01	0.00	0.02	0.09	0.01	0.00	0.00	0.02
Mg	0.30	2.40	0.45	0.37	0.00	0.39	2.12	0.38	0.42	0.00
Ca	0.70	0.16	0.54	0.00	1.97	0.87	0.08	0.49	0.00	2.00
Na	0.01	1.83	0.45	0.09	0.00	0.01	1.92	0.52	0.05	0.00
K	0.00	0.00	0.00	0.89	0.00	0.00	0.01	0.00	0.90	0.00
Sum	8.00	15.02	4.00	7.03	8.01	8.00	15.03	4.00	7.00	8.01
X_{alm}	64.41					55.51				
X_{grs}	23.24					28.58				
X_{prp}	9.93					13.00				
X_{sps}	2.42					2.90				
$X_{Mg\,(gl)}$		0.76					0.68			
X_{jd}			0.34					0.36		
X_{acm}			0.11					0.16		
$X_{wo,en,fs}$			0.55					0.48		
X_{ep}					0.19					0.24

Table 3. Representative mineral composition from Blueschist SYNS03a and eclogite SYNS04a, in weight percentage of oxides and atomic proportions. With chosen endmembers proportions: garnets X_{alm}, X_{grs}, X_{prp}, X_{sps}; amphibole $X_{\mathbf{mg}(gl)}$; pyroxene X_{jd}, X_{acm}, $X_{wo,en,fs}$; and epidote X_{ep}.

Clinopyroxene

The clinopyroxenes observed were exclusively omphacite in both blueschist (SYNS03) and eclogite (SYNS04). The compositions of the omphacites are similar and no zoning was observed (Figure 11b).

Amphiboles

The type of amphibole observed in all three rocks (eclogite, blueschist and greenschist) is glaucophane of similar compositions (Figure 11c). The crystals observed lacked any observable zoning. Thus it appears that little or no replacement of glaucophane by actinolite occurred which is unusual for greenschist facies retrogression.

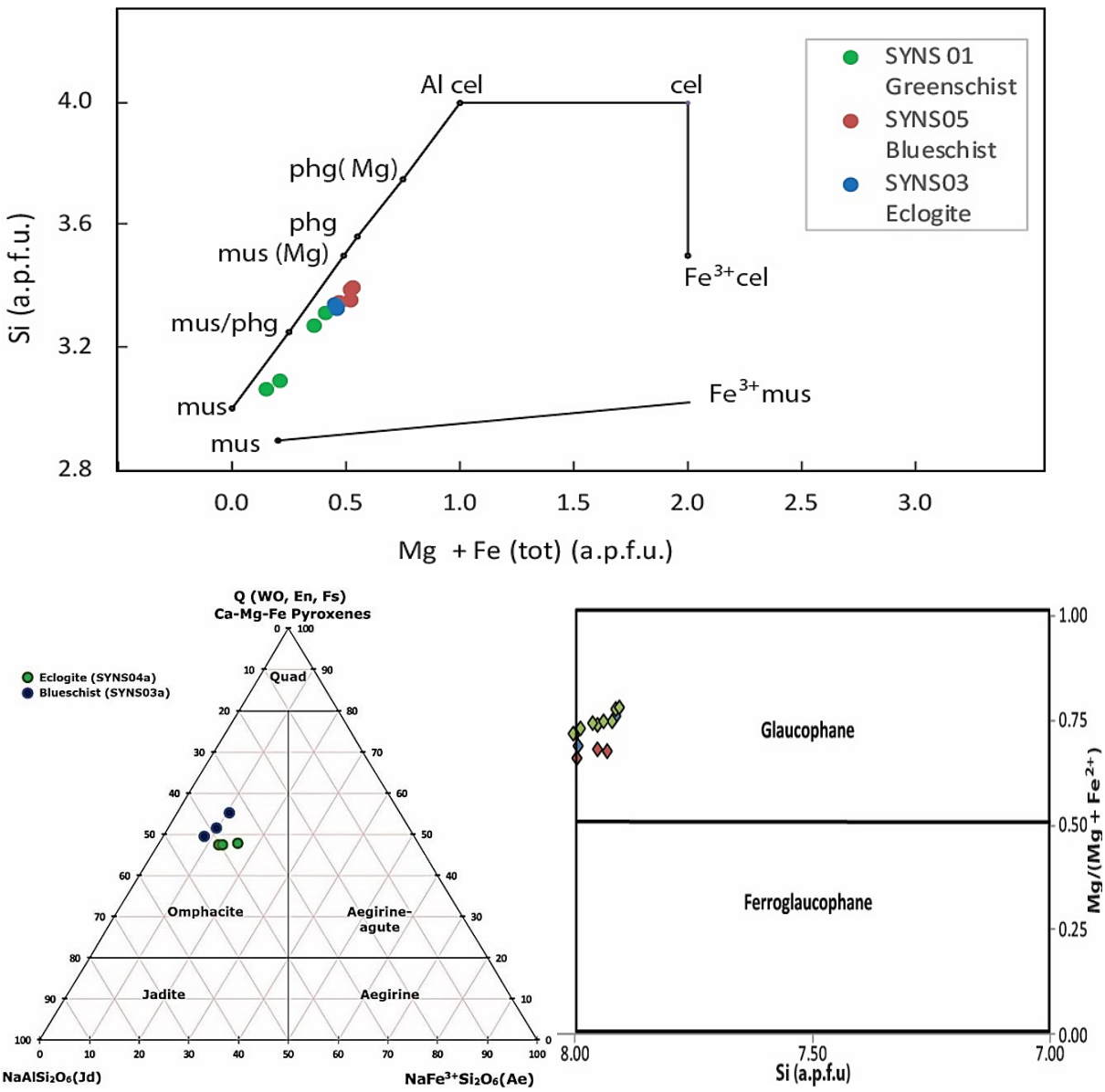

Figure 11. a) The white mica from greenschist, blueschist and eclogite classified in terms of Si vs Mg +Fe (tot) a.p.f.u. (Tischendorf et al., 2004). b) Ternary diagram (Morimoto, 1988) showing the clinopyroxene composition of SYNS03a and SYNS04a. c) Composition of amphibole of SYNS01 (green), SYN03a (blue) and SYNS04a (red). In Si v. Mg/(Mg+Fe^{2+}) after Leake et al. (1997).

Epidote

Epidote crystals in the studied samples are zoned (e.g. Figure 8d). Epidote content was expressed as $X_{ep} = Fe^{3+}/(Fe^{3+}+Al+Mn)$. From core to rim, X_{ep} increases from ~ 0.10 to ~ 0.30. In the eclogite parts of thin sections SYNS03a and b, porphyroblasts of zoisite are present. In these samples, clinozoisite content was expressed as $X_{cz} = (Al -2)/(Al + Cr + Fe^{3+} - 2)$ after Franz and Liebscher (2004). In these samples, $X_{cz} = 0.93$.

Garnets

There are garnets present in all samples which are variably preserved. The garnets in the eclogite (SYNS04 a and b) are large (~2.5 mm in diameter) and euhedral. The garnets in SYNS03 (a and b) are found along the boundary between the eclogite and blueschist. Their sizes range from 1 to 2 mm. Larger garnets are fractured, whereas smaller garnets are intact. The garnets in the greenschists (SYNS01 and SYNS02) are small (~1 mm in diameter) and highly fractured. Two garnet profile were taken: one in SYNS01 and one in SYNS04a. The garnets in SYNS01 (Figure 12a) are homogeneous with respect to almandine content with X_{alm} = ~63% and grossular content with X_{Grs} = ~22%, whereas the concentration of pyrope increase from X_{Pyp} = 7.3 in garnet cores to X_{Pyp} =11.6 % in garnet rims. There is a corresponding decrease in spessartine concentration from X_{Sps} 8.2 to 1.5% (Figure 12a). The garnet in sample SYNS04a shows three stages of growth: core (~1-1.8 mm), inner rim (~0.2-1 mm and ~1.8-2.1 mm) and outer rim (~0-0.2 and ~2.1-2.5). From its core to its inner rim and then its outer rim, the garnet composition changes: almandine X_{Alm} ~57-64-57%; grossular X_{Grs} ~21-25-28%; pyrope X_{Pyp} = ~6-11-12%; and spessartine X_{Sps} ~15-4-3%.

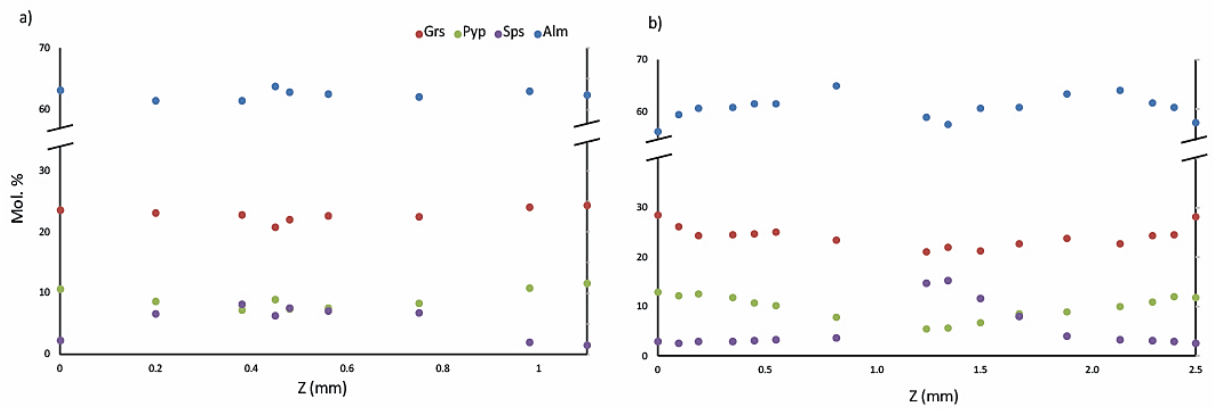

Figure 12. Profiles across garnet porphyroblasts in a) greenschist sample SYNS01 and b) eclogite sample SYNS04a. Displacing the weight proportions of garnet endmembers: grossular (grs), pyrope (pyp), spessartine (sps) and almandine (alm).

Average P-T calculations

The average pressure and temperature (average P-T) were estimated using garnet rims and matrix compositions for eclogite (SYNS04a) blueschist (SYNS03a) and greenschist (SYNS01) (Table 3). The reason for using the garnet rim and matrix composition is to obtain a P-T estimates for last stable mineral assemblage.

From the eclogite (SYNS 04a) a P-T estimate of 555 ± 37°C and 2.04 ± 0.22 GPa was obtained for the garnet rim and matrix assemblage of omphacite, glaucophane, phengite, epidote and rutile. From the blueschist (SYNS03a), a P-T estimate of 513 ± 37 °C, and 1.59 ± 0.18 GPa was obtained for the garnet rim and matrix assemblage of omphacite, glaucophane, phengite, epidote and rutile. The greenschist sample SYNS01 did not yield a meaningful P-T estimate, probably because of disequilibrium.

Discussion

The preservation of the HP-LT rocks at the study site (Figure 4) could be caused by one or a combination of the following factors: different P-T conditions, fluid-rock interaction and/or bulk composition differences. These factors and how they may have affected the studied rock sequence will be discussed in the following sections.

Eclogite and Blueschist

The first step of this analysis is to determine the relationship between the eclogite sample SYNS04a and blueschist SYNS03a. For each of these samples, average P-T conditions were estimated from the matrix minerals and garnet rim compositions. For the blueschist sample SYNS03a, an average P-T estimate of 1.59 ± 0.18 GPa and 513 ± 37 °C was obtained. For the eclogite sample SYNS04a, an average P-T estimate of 2.04 ± 0.22 GPa and 555 ± 37 °C was obtained. There is thus a significant difference in P-T conditions between the two rocks. The average P-T estimate obtained from the eclogite sample SYNS04a is similar to that which was obtained from garnet inner rims in eclogites and blueschists at Fabrika (Skelton, et al., 2019) (Figure 13). The average P-T estimate obtained from the blueschist sample is similar to that which was obtained from the matrix and garnet rim from the same layered rocks by Skelton et al. (2019) (Figure 13). The similarities between these estimates suggests that similar metamorphic states are recorded by the eclogite and blueschist in the present study. In conclusion, I argue that the eclogite and blueschist experienced peak metamorphism at ~2.0 GPa and ~550 °C and that the blueschist records retrogression below 1.6 GPa and 510°C (Figure 13). The P-T path roughly overlaps the results of Skelton et al. (2019) (Figure 13). On the other hand, the eclogite sample SYNS04a retains its high P assemblage, implying that it was not been retrogressed at blueschist facies conditions. Possible causes of this preservation will be discussed below.

One possible reason for preservation of eclogite can be its bulk composition, i.e. that its original eclogite facies minerals were also stable at blueschist facies conditions. Coexisting eclogite and blueschist in rocks of different compositions has been describe previously (Beinlich et al., 2010; Brovarone et al., 2011; Wei and Clarke, 2011; Skelton et al., 2019). For example, Skelton et al. (2019) found that high Fe_2O_3, Al_2O_3 and K2O favoured eclogite assemblage and high Na_2O and MgO favoured blueschist assemblage. For the blueschist sample SYNS03 and eclogite sample SYNS04 the opposite is largely true (Table 2, Figure 14). The weight percentage

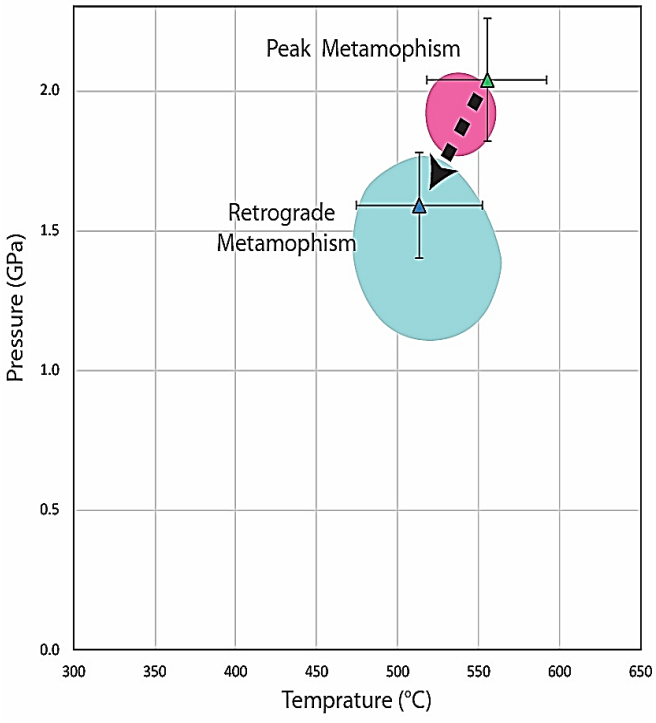

Figure 13. Average P-T estimations of eclogite sample SYNS04a (green triangle) and blueschist sample SYNS03a (blue triangle). Plotted with P-T estimation from Skelton et al. (2019): estimated field of peak metamorphism pink field and retrograde metamorphism blue field. Arrow indicating the suggested P-T path of the rocks.

of Al_2O_3 and Fe_2O_3 are higher in the blueschist, and although the concentration of MgO is higher in the blueschist, the concentration of Na_2O is lower (Figure 14). Also, in contrast to the interlayered eclogite and blueschist studied by Skelton et al. (2019) which differ in major elements concentrations by up to five times, the chemical compositions of the eclogite SYNS04 and blueschist SYNS03 are comparatively similar (Table 2). The ratio of $X_{Na2O} = Na_2O/(Na_2O + CaO)$ has been put forward as an explanation for the coexistence of eclogite and blueschist by Gomez-Pugnarie et al. (1997). They showed that high X_{Na2O} values favour blueschist and low values favour eclogite. However, the blueschist sample SYNS03 has an X_{Na2O} value of 0.292 whereas the eclogite sample SYNS04 has an X_{Na2O} value of 0.310. Thus, this explanation is not supported by the data. Brovarone et al. (2011) found that the CaO content rather than Na_2O content controlled eclogite preservation. They showed that higher X_{CaO}= CaO/(CaO + FeO) favored eclogite. Noting that FeO(total) = Fe_2O_3(total) * 0.89981, the blueschist SYNS03 has an X_{CaO} value of 0.51 whereas the eclogite SYNS04 has an X_{CaO} values of 0.63. Thus coexistence of eclogite and blueschist could have been caused by differences in X_{CaO}.

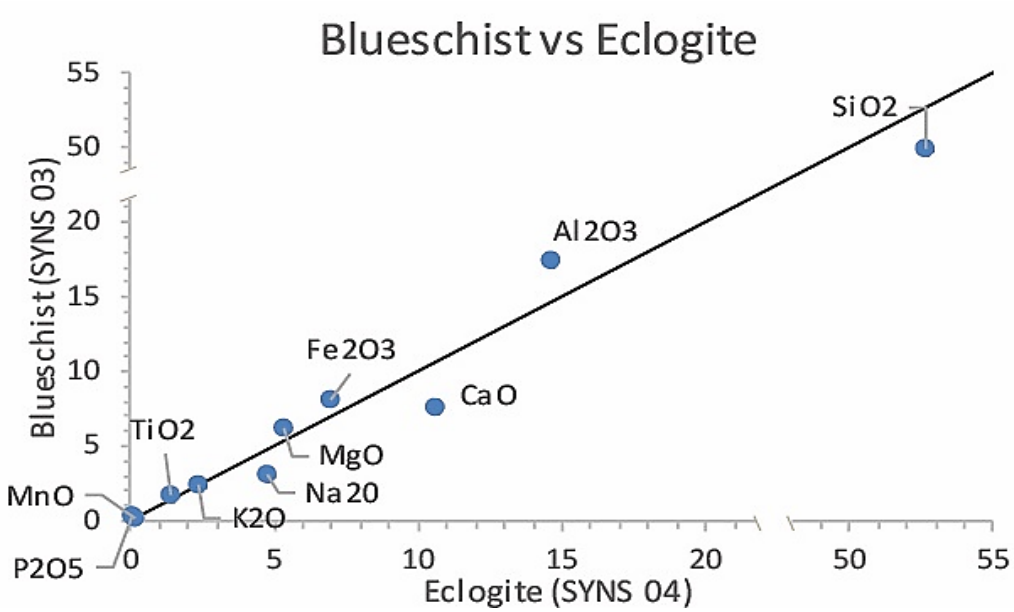

Figure 14. Isocon diagrams of the blueschist and eclogite oxide concentrations compared, the black line displays 1:1 ratio. The ratio line is put at the 1:1 ratio instead of through the immobile elements TiO_2 and Al_2O_3 as the rocks are not determined to have the same origin. The plot is instead focused on visualizing the chemical differences between the eclogite and blueschist.

However, with the exception of small differences in X_{CaO}, the eclogite (SYNS04) and blueschist (SYNS03) have similar the major element concentrations (Table 2). This similarity suggests a common protolith. To verify this, I have compared immobile and mobile element concentrations (Figure 15a). If the blueschist and eclogite have a common protolith, their immobile element concentrations should be similar. Figure 15a shows considerable differences in immobile element concentrations (REEs, U, Nb Ti, Th and Zr) between the eclogite and blueschist. This argues against a common protolith. The ratio of the immobile elements Ti, Al and Nb are above 1, and ratio of REEs, Th and U are far below 1 (Figure 15a). The differences cannot be explained by a volume change, as this would not affect ratios. Experimental tests have shown that the REEs can be mobilized during subduction (Tsay et al., 2014). However, different degrees of mobility would be expected (Tsay et al., 2014) but is not observed (Figure 15a). The differences in immobile elements shows that the blueschist and eclogite had slightly

different protolith despite similar major element concentrations. The notion of the whole sequence once was completely homogeneous is therefore discarded.

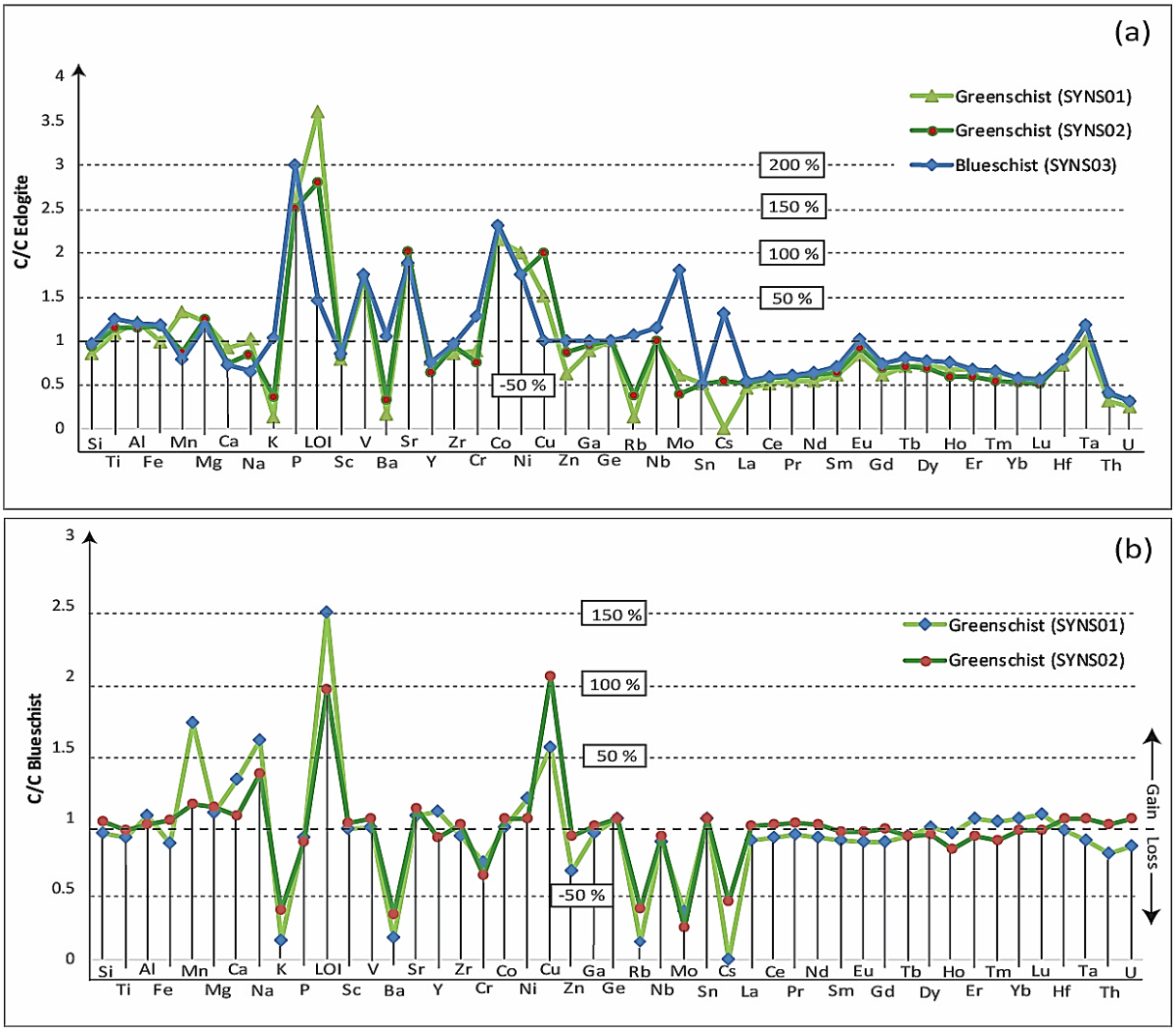

Figure 15. Concentration plots comparing the chemistry of by dividing the element concentrations of the altered rocks, by the least altered. The a) the eclogite is assumed to be least the altered, dividing the blueschist and greenschists by its composition. Resulting in values of relative differences between eclogite and the other rocks, a value of 1 means same concentration. There appear to be relation between the blueschist and greenschists as they mostly follow same trend. The b) assumes the blueschist is the least altered. The greenschists values of immobile elements are both at around values of 0.9 forming a baseline. Indicating a volume increase of 10% from blueschist to greenschists.

The protoliths for the eclogite, blueschist and impure metasandstone can be estimated from their bulk chemistry. The impure metasandstone was a sedimentary sandstone layer, assumed from the high silica content (Table 2). The blueschist has high concentrations of majors Al, Mg and Fe, with minors Co, Ni and Cu (Table 2). The chemistry fits with values expected for volcaniclastic sediments e.g. ach layers.

The eclogite sample SYNS04 and the eclogite part of sample SYN03 have different modes (Figure 16). Sample SYNS03 contains less anhydrous omphacite but more hydrous phengite (Figure 16 a and c). The change implies hydration of the eclogite in contact with blueschist. Fluid flow along the eclogite/blueschist contact can also be inferred from a phengite rich zone in the eclogite (Figure 7). Thus fluid hydrated parts of the eclogite causing the forming of phengite in a less than 2 cm wide zone at its margin. The limited extent of hydration could be

a mechanical effect of low permeability in the eclogite compared with high permeable in the blueschist, as may also be the case for eclogite knockers on Syros (Ague, 2007). The blueschist could have channelized the fluid leading to adjacent rock volumes being comparatively dry (cf. Breeding et al., 2003). This interpretation is further corroborated by the higher average P-T estimates made for the eclogite. The absence of re-equilibration can thus reflect a lack of fluid (Proyer, 2003; Schorn, 2018).

The profiles of garnet from eclogite SYNS05a and greenschist SYNS01 are interpreted to have formed during prograde metamorphism. As the core is spessartine rich with decreasing concentration towards the rim, coupled with an increase of pyrope concentration towards the rim. The garnet in the eclogite shows no sign of retrograde growth. This also supports the idea that the eclogite experience little or no retrogression.

Blueschist and greenschist

There are clear similarities of chemistry and mineralogy between the greenschist samples SYNS 01 and SYNS02 and the blueschist sample SYNS 03 (Table 2). The presence of (partly replaced) glaucophane in SYNS01 and SYNS02 is a clear indication of former blueschist facies metamorphism (Figure 5a & 6a). Glaucophane in the most retrogressed sample, SYNS01, lacks zoning or replacement by actinolite. This observation as well as observed preservation of prograde garnet and phengite imply that greenschist facies retrogression was limited in these samples.

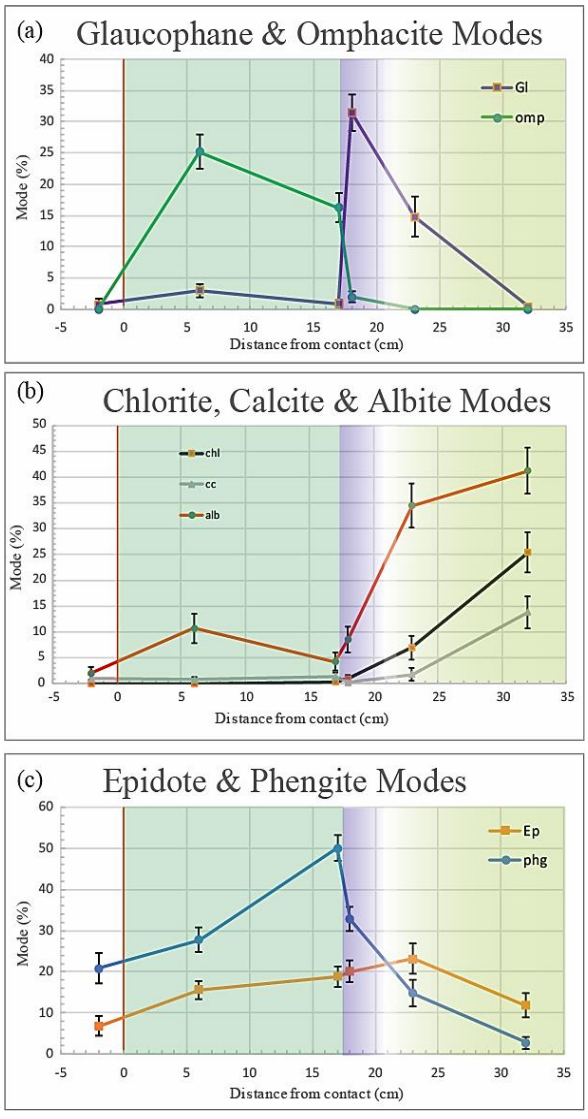

Mineralogical and chemical similarities suggest that the blueschist and greenschist formed from the same rock and that this rock was metamorphosed at blueschist facies conditions and thereafter partly retrogressed at greenschist facies conditions. This implies that the blueschist and greenschist have the same protolith, which can be tested (Figure 15b). The concentration of Ti, Al, Zr, Th and the light REEs are the same for both rock types. These elements plot at 0.9 on a C/C plot in Figure 15b indicating volume gain of ca. 10% (Ague, 2003), caused by dilution. The greenschists are depleted in the mobile LILE elements K, Ba, Rb, Mo and Cs, but not Ca and Sr, perhaps due to fluid-rock interaction.

Figure 16. Mineral mode of the 7 different samples plotted against the distance from eclogite- impure metasandstone contact. The mineral mode is calculated by point counting with standard error according method of Vanderplas and Tobi. (1965). The different field indicated by colour roughly represent the extent of the various rock units going from left to right: white impure metasandstone, dark green eclogite, blue blueschist and light green greenschist.

The mineralogical differences between the greenschists and blueschist are illustrated in Figure 16. The modes of glaucophane and phengite decreases from the blueschist to greenschists and there is a corresponding increase in the modes of chlorite, carbonate and albite (Figure 16b). The differences in the degree of greenschist facies overprinting correlates inversely with distance from the impure metasandstone.

The changes in mineral mode from the blueschist to the greenschists suggest that glaucophane, phengite and epidote are replaced by chlorite, carbonate and albite by (e.g.) the following generalized reaction (Figure 16).

Glaucophane + Phengite + Epidote + H_2O + CO_2 → Chlorite + Calcite + Albite.

This reaction implies loss of K; a further indication that greenschist facies overprinting is partly metasomatic.

Preservation of HP rocks

The preservation of blueschist and eclogite was likely caused by at least one of these three factors: I) fluids flow in or along the impure metasandstone, stabilizing the rocks similar to Kleine et al. (2014); II) Distance from the fault, located south of the outcrop (Figure 2); the fault could have channelized the fluids, altering the rocks in the vicinity; III) protection from fluids by the possibly impermeable impure metasandstone layer (Matthews and Schliestedt, 1984). Kleine et al. (2014) showed that a CO_2 rich fluid could stabilize blueschist facies rocks during retrogression. This cannot be the case as greenschists samples SYNS01 and SYN02, because these contain more carbonate than the blueschist sample SYNS03, implying that carbonation of the samples occurred during retrogression. The hypothesis of a fluid stabilizing high PT assemblages is therefore considered unlikely for these rocks. The contacts between eclogite, blueschist and greenschist are sub-horizontal whereas the fault zone is sub-vertical implying the fluid flow channelizing along the fault cannot have stabilized the HP assemblages. Theses contacts are however parallel to the base on the impure metasandstone, i.e. metamorphic zonation is a function of distance from this boundary. The impure metasandstone could have prevented fluids from affecting the rock sequence, explaining the high degree of preservation immediately beneath it. A similar scenario have been described at neighbouring island Tinos by Breeding et al. (2003).

Conclusions

I conclude that:

I) The eclogite formed at ~2.0 GPa and ~550 °C during peak metamorphism and the blueschist formed during retrogression at ~1.6 GPa and ~510 °C.
II) The eclogite is extremely well preserved as the impure metasandstone protected it from later fluid interaction during retrogression.
III) The blueschist is partly replaced under greenschist facies by metasomatism during hydration and carbonation. The preservation of blueschist caused partial protection from fluid by the impure metasandstone.
IV) The average pressure and temperature of the eclogite and blueschist overlaps with P-T estimation of Skelton et al. (2019).
V) The compositions of the rocks are similar fitting the characteristics expected for volcanoclastic sediments.

Acknowledgement

I would like to thank my supervisor Alasdair Skelton for the opportunity to do this project, the counselling throughout the project and the extra help refining the text. A special thanks to Alexandre Peillod for counsel and engagement throughout the whole project. I greatly thank Muriel Erambert at Oslo University for her professional and personal supervision during the EMPA analyses, and for finishing the garnet profiles. I thank Paola Manzotti for the introduction to the program Theriak-Domino (psudo-section) and counselling. I thank Francesco Nosenzo for counsel and Nicole Flanders for correcting parts of the report. I thank Arne Lif and Björn Eriksson for their technical help.

I would also like to thank the other master students for the discussions and for inspiration emitted throughout the year. A special thanks to my partner Emma Sivertsson for helping to correct the report and supporting me throughout the project.

References

Ague, J.J., 2003. Fluid infiltration and transport of major, minor, and trace elements during regional metamorphism of carbonate rocks, Wepawaug Schist, Connecticut, USA. Am. J. Sci. 303, 753–816. https://doi.org/10.2475/ajs.303.9.753

Ague, J.J., 2007. Models of permeability contrasts in subduction zone mélange: Implications for gradients in fluid fluxes, Syros and Tinos Islands, Greece. Chem. Geol., Geochemical processes responsible for element mobility from the slab to the surface 239, 217–227. https://doi.org/10.1016/j.chemgeo.2006.08.012

Aubouin, J., 1957. Essai de correlations stratigraphiques en Grece occidentale. Bull. Société Géologique Fr. S6-VII, 281–304. https://doi.org/10.2113/gssgfbull.S6-VII.4-5.281

Beinlich, A., Klemd, R., John, T., Gao, J., 2010. Trace-element mobilization during Ca-metasomatism along a major fluid conduit: Eclogitization of blueschist as a consequence of fluid-rock interaction. Geochim. Cosmochim. Acta 74, 1892–1922. https://doi.org/10.1016/j.gca.2009.12.011

Bonneau, M., 1984. Correlation of the Hellenide nappes in the south-east Aegean and their tectonic reconstruction. Geol. Soc. Spec. Publ. 17, 517–527. https://doi.org/10.1144/GSL.SP.1984.017.01.38

Breeding, C.M., Ague, J.J., Bröcker, M., Bolton, E.W., 2003. Blueschist preservation in a retrograded, high-pressure, low-temperature metamorphic terrane, Tinos, Greece: Implications for fluid flow paths in subduction zones. Geochem. Geophys. Geosystems 4. https://doi.org/10.1029/2002GC000380

Bröcker, M., Baldwin, S., Arkudas, R., 2013. The geological significance of 40Ar/39Ar and Rb–Sr white mica ages from Syros and Sifnos, Greece: a record of continuous (re)crystallization during exhumation? J. Metamorph. Geol. 31, 629–646. https://doi.org/10.1111/jmg.12037

Brovarone, A.V., Groppo, C., Hetényi, G., Compagnoni, R., Malavieille, J., 2011. Coexistence of lawsonite-bearing eclogite and blueschist: Phase equilibria modelling of Alpine Corsica metabasalts and petrological evolution of subducting slabs. J. Metamorph. Geol. 29, 583–600. https://doi.org/10.1111/j.1525-1314.2011.00931.x

Cliff, R.A., Bond, C.E., Butler, R.W.H., Dixon, J.E., 2017. Geochronological challenges posed by continuously developing tectonometamorphic systems: insights from Rb–Sr mica ages from the Cycladic Blueschist Belt, Syros (Greece). J. Metamorph. Geol. 35, 197–211. https://doi.org/10.1111/jmg.12228

England, P., Molnar, P., 1990. Surface uplift, uplift of rocks, and exhumation of rocks. Geology 18, 1173–1177. https://doi.org/10.1130/0091-7613(1990)018<1173:SUUORA>2.3.CO;2

Ernst, W.G., 1988. Tectonic history of subduction zones inferred from retrograde blueschist P-T paths. Geology 16, 1081–1084. https://doi.org/10.1130/0091-7613(1988)016<1081:THOSZI>2.3.CO;2

Faccenna, C., Jolivet, L., Piromallo, C., Morelli, A., 2003. Subduction and the depth of convection in the Mediterranean mantle. J. Geophys. Res. Solid Earth 108, ETG 9-1-9-13.

Franz, G., Liebscher, A., 2004. Physical and Chemical Properties of the Epidote Minerals–An Introduction–. Rev. Mineral. Geochem. 56, 1–81. https://doi.org/10.2138/gsrmg.56.1.1

Fytikas, M., Innocenti, F., Manetti, P., Peccerillo, A., Mazzuoli, R., Villari, L., 1984. Tertiary to Quaternary evolution of volcanism in the Aegean region. Geol. Soc. Spec. Publ. 17, 687–699. https://doi.org/10.1144/GSL.SP.1984.017.01.55

Holland, T.J.B., Powell, R., 2011. An improved and extended internally consistent thermodynamic dataset for phases of petrological interest, involving a new equation of

state for solids. J. Metamorph. Geol. 29, 333–383. https://doi.org/10.1111/j.1525-1314.2010.00923.x
Jacobshagen, V., Dornsiepen, U., Giese, P., Wallbrecher, E., 1986. Geologie von Griechenland. Borntraeger, Berlin.
Jolivet, L., Faccenna, C., Huet, B., Labrousse, L., Le Pourhiet, L., Lacombe, O., Lecomte, E., Burov, E., Denèle, Y., Brun, J.-P., Philippon, M., Paul, A., Salaün, G., Karabulut, H., Piromallo, C., Monié, P., Gueydan, F., Okay, A.I., Oberhänsli, R., Pourteau, A., Augier, R., Gadenne, L., Driussi, O., 2013. Aegean tectonics: Strain localisation, slab tearing and trench retreat. Tectonophysics 597–598, 1–33. https://doi.org/10.1016/j.tecto.2012.06.011
Keiter, M., Ballhaus, C., Tomaschek, F., 2011. A New Geological Map of the Island of Syros (Aegean Sea, Greece): Implications for Lithostratigraphy and Structural History of the Cycladic Blueschist Unit. Geological Society of America.
Kleine, B, Skelton, A, Huet, B, Pitcairn,I, 2014. Preservation of blueschist-facies minerals along a shear zone by coupled metasomatism and fast-flowing CO2-bearing fluids. J. Petrol. 1905. https://doi.org/10.1093/petrology/egu045
Leake, B.E., Woolley, A.R., Arps, C.E.S., Birch, W.D., Gilbert, M.C., Grice, J.D., Hawthorne, F.C., Kato, A., Kisch, H.J., Krivovichev, V.G., Linthout, K., Laird, J., Mandarino, J., Maresch, W.V., Nickel, E.H., Rock, N.M.S., Schumacher, J.C., Smith, D.C., Stephenson, N.C.N., Ungaretti, L., Whittaker, E.J.W., Youzhi, G., 1997. Nomenclature of amphiboles: Report of the subcommittee on amphiboles of the international mineralogical association commission on new minerals and mineral names. Mineral. Mag. 61, 295–321.
Maluski, H., Bonneau, M., Kienast, J.R., 1987. Dating the metamorphic events in the Cycladic area; ^{39} Ar/ ^{40} Ar data from metamorphic rocks of the Island of Syros (Greece). Bull. Société Géologique Fr. III, 833–842. https://doi.org/10.2113/gssgfbull.III.5.833
Matthews, A., Schliestedt, M., 1984. Evolution of the blueschist and greenschist facies rocks of Sifnos, Cyclades, Greece - A stable isotope study of subduction-related metamorphism. Contrib. Mineral. Petrol. 88, 150–163. https://doi.org/10.1007/BF00371419
Morimoto, N., 1988. Nomenclature of Pyroxenes. Mineral. Petrol. 39, 55–76. https://doi.org/10.1007/BF01226262
Nisbet, E.G., Dietrich, V.J., Esenwein, A., 1979. Routine trace element determination in silicate minerals and rocks by X-ray fluorescence. Fortschritte Mineral. 57, 264–279.
Norrish, K., Hutton, J.T., 1969. An accurate X-ray spectrographic method for the analysis of a wide range of geological samples. Geochim. Cosmochim. Acta 33, 431–453. https://doi.org/10.1016/0016-7037(69)90126-4
Pe-Piper, G., Piper, D.J.W., Matarangas, D., 2002. Regional implications of geochemistry and style of emplacement of Miocene I-type diorite and granite, Delos, Cyclades, Greece. Lithos 60, 47–66. https://doi.org/10.1016/S0024-4937(01)00068-8
Platt, J.P., 1993. Exhumation of high-pressure rocks: a review of concepts and processes. Terra Nova 5, 119–133. https://doi.org/10.1111/j.1365-3121.1993.tb00237.x
Poli, S., Schmidt, M.W., 2002. Petrology of subducted slabs. Annu. Rev. Earth Planet. Sci. 30, 207–235. https://doi.org/10.1146/annurev.earth.30.091201.140550
Powell, R., Holland, T., 1994. Optimal geothermometry and geobarometry. Am. Mineral. 79, 120–133.
Proyer, A., 2003. The preservation of high-pressure rocks during exhumation: Metagranites and metapelites. Lithos 70, 183–194. https://doi.org/10.1016/S0024-4937(03)00098-7

Ricou, L.-E., Burg, J.-P., Godfriaux, I., Ivanov, Z., 1998. Rhodope and Vardar: The metamorphic and the olistostromic paired belts related to the Cretaceous subduction under Europe. Geodin. Acta 11, 285–309. https://doi.org/10.1016/S0985-3111(99)80018-7

Ring, U., Brandon, M.T., Willett, S.D., Lister, G.S., 1999. Exhumation processes. Geol. Soc. Spec. Publ. 154, 1–27. https://doi.org/10.1144/GSL.SP.1999.154.01.01

Ring, U., Glodny, J., Will, T., Thomson, S., 2010. The hellenic subduction system: High-pressure metamorphism, exhumation, normal faulting, and large-scale extension. Annu. Rev. Earth Planet. Sci. 38, 45–76. https://doi.org/10.1146/annurev.earth.050708.170910

Royden, L.H., Husson, L., 2006. Trench motion, slab geometry and viscous stresses in subduction systems. Geophys. J. Int. 167, 881–905. https://doi.org/10.1111/j.1365-246X.2006.03079.x

Schorn, S., 2018. Dehydration of metapelites during high-P metamorphism: The coupling between fluid sources and fluid sinks. J. Metamorph. Geol. 36, 369–391. https://doi.org/10.1111/jmg.12296

Schumacher, J.C., Brady, J.B., Cheney, J.T., Tonnsen, R.R., 2008. Glaucophane-bearing marbles on Syros, Greece. J. Petrol. 49, 1667–1686. https://doi.org/10.1093/petrology/egn042

Skelton, A., Peillod, A., Glodny, J., Klonowska, I., Månbro, C., Lodin, K., Ring, U., 2019. Preservation of high-P rocks coupled to rock composition and the absence of metamorphic fluids. J. Metamorph. Geol. 0. https://doi.org/10.1111/jmg.12466

Thomson, S.N., Stöckhert, B., Brix, M.R., 1998. Thermochronology of the high-pressure metamorphic rocks of Crete, Greece: Implications for the speed of tectonic processes. Geology 26, 259–262. https://doi.org/10.1130/0091-7613(1998)026<0259:TOTHPM>2.3.CO;2

Tischendorf, G., Rieder, M., Förster, H.J., Gottesmann, B., Guidotti, Ch.V., 2004. A new graphical presentation and subdivision of potassium micas. Mineral. Mag. 68, 649–667. https://doi.org/10.1180/0026461046840210

Tomaschek, F., Kennedy, A.K., Villa, I.M., Lagos, M., Ballhaus, C., 2003. Zircons from Syros, Cyclades, Greece - Recrystallization and mobilization of zircon during high-pressure metamorphism. J. Petrol. 44, 1977–2002.

Tsay, A., Zajacz, Z., Sanchez-Valle, C., 2014. Efficient mobilization and fractionation of rare-earth elements by aqueous fluids upon slab dehydration. Earth Planet. Sci. Lett. 398, 101–112. https://doi.org/10.1016/j.epsl.2014.04.042

van Hinsbergen, D.J.J., Hafkenscheid, E., Spakman, W., Meulenkamp, J.E., Wortel, R., 2005a. Nappe stacking resulting from subduction of oceanic and continental lithosphere below Greece. Geology 33, 325–328. https://doi.org/10.1130/G20878.1

Vanderplas, L., Tobi, A., 1965. A Chart for Judging Reliability of Point Counting Results. Am. J. Sci. 263, 87-+.

Wei, C.J., Clarke, G.L., 2011. Calculated phase equilibria for MORB compositions: A reappraisal of the metamorphic evolution of lawsonite eclogite. J. Metamorph. Geol. 29, 939–952. https://doi.org/10.1111/j.1525-1314.2011.00948.x

Appendix

	carb	SD	Ep	SD	Gl	SD	phg	SD	chl	SD	alb	SD	grt	SD	omp	SD	Qtz	SD	Other	SD
SYNS01	13.8	3.1	11.8	2.9	0.4	0.6	2.8	1.5	25.4	3.9	41.2	4.4	0.4	0.6	-	-	-	-	4.2	1.8
SYNS02	1.8	1.2	23.2	3.8	14.8	3.2	14.8	3.2	7.2	2.3	34.4	4.25	0.0	0.0	-	-	-	-	4.0	1.8
SYNS03 B	0.3	0.3	20.1	2.5	31.5	2.9	32.7	3.0	1.0	0.6	8.6	1.8	1.0	0.6	1.9	0.9	-	-	3.3	1.1
SYNS03 E	1.4	0.7	18.8	2.5	0.9	0.6	50.1	3.2	0.4	0.4	4.3	1.3	0.8	0.6	16.2	2.3	-	-	1.3	0.7
SYNS04 a & b	0.8	0.6	15.6	2.3	3.0	1.1	27.8	2.8	-	-	10.7	2.0	8.3	1.7	30.1	2.9	-	-	3.7	1.2
SYNS05	1.0	0.9	6.8	2.3	0.8	0.8	20.8	3.6	-	-	2.0	1.3	0.6	0.7	-	-	64.2	4.3	2.2	1.3

Appendix 1. Mineral mode of the different rocks determined by point counting, with calculated standard deviation (Van der Plas and Tobi, 1965). The data for SYN03 a and b blueschist part is combined to SYNS03 B and eclogite SYNS03 E.